Letter

Disorder-induced dynamical Griffiths singularities after certain quantum quenches

José A. Hoyos [1,2], R. F. P. Costa [3], and J. C. Xavier [3]

[1]*Instituto de Física de São Carlos, Universidade de São Paulo, C.P. 369, São Carlos, São Paulo 13560-970, Brazil*

[2]*Max Planck Institute for the Physics of Complex Systems, Nöthnitzer Strasse 38, 01187 Dresden, Germany*

[3]*Instituto de Física, Universidade Federal de Uberlândia, C.P. 593, 38400-902 Uberlândia, MG, Brazil*

(Received 30 January 2022; accepted 30 September 2022; published 10 October 2022)

We demonstrate that in a class of disordered quantum systems the dynamical partition function is not an analytical function in a time window after certain quantum quenches. We related this behavior to rare and large regions with atypical inhomogeneity configurations. We also quantify the strength of the associated singularities and their signatures in experiments and numerical studies.

DOI: 10.1103/PhysRevB.106.L140201

Phase transitions (PTs) are among the most intriguing phenomena in nature. When crossed, the macroscopic properties of matter change fundamentally, often requiring new concepts for a proper description [1]. In thermodynamic equilibrium, PTs are on firm theoretical grounds as they occur whenever a zero of the partition function touches the real-temperature (or field) axis [1,2]. Consequently, thermodynamic observables become nonanalytic functions of temperature/field at the transition point. Notably, these Yang-Lee-Fisher (YLF) zeros were recently measured experimentally [3,4].

Inhomogeneities, which are nearly ubiquitous in experiments, play an important role in equilibrium PTs. For instance, even the smallest amount of them can change the singularities of a critical system [5], smear the PT [6,7], or even destroy it [8]. Another remarkable inhomogeneity-induced phenomenon is the stabilization of a Griffiths phase (GP): an extended region in the phase diagram surrounding a phase-transition manifold where the free energy is nonanalytic [9,10]. Counterintuitively, the nonanalyticity is due to so-called rare regions (RRs)—large and rare regions in space with atypical configurations of inhomogeneities—which provide YLF zeros arbitrarily close to the real-temperature axis [9,11,12].

Over the past decades, the influence of the RRs on many observables has been quantified in a multitude of strongly interacting systems ranging from classical and quantum models in equilibrium to nonequilibrium reaction-diffusion models (for reviews, see Refs. [13–15]). In the associated GPs, the RRs endow many observables with singular behavior in the long-time/low-frequency regime. This common feature is due to the RRs' long relaxation times [16–20].

With the growing capacity of experimentally accessing the time evolution of closed quantum many-body systems [21,22], it then became natural to inquire whether the RRs play any important role in their time evolution. Clearly, the notion of slow RRs at equilibrium does not apply and thus their importance cannot be anticipated. Evidently, obtaining a result on the RR effects in a general out-of-equilibrium situation is desirable but very unlikely to exist. We thus restrict ourselves to the simpler case of quantum quenches which already allows the study of fundamental phenomena such as entanglement spreading and thermalization [23–25]. Here, the system's initial state is $|\psi_0\rangle$, the ground state of $H_0 \equiv H(h_0)$, and time evolved according to the postquench Hamiltonian $H \equiv H(h)$, with h being a tuning parameter. In this context, the concept of dynamical quantum phase transitions (QPTs) is quite useful [26] because an analogy with equilibrium PTs can be made. The linking quantity is the dynamical free energy

$$f(t) = -V^{-1} \ln |Z(t)|^2, \tag{1}$$

where $Z(z) = \langle\psi_0|e^{-iHz}|\psi_0\rangle$ is the return probability amplitude after the quench, $z = t + i\tau$ is the complex time, and V is the system volume. Z is the dynamical analog of the equilibrium partition function. As in equilibrium PTs, its zeros accumulate in lines or areas on the complex-time plane and, in the thermodynamic limit, may touch the real-time axis. When this happens, a dynamical QPT occurs [26–32] and has been experimentally verified in different quantum simulator platforms [33–37] (for a review, see Ref. [38]).

In this Letter, we use the unifying concept of YLF zeros to show that the RRs dominate the system's early-time dynamics for all quenches which do not cross the bulk equilibrium QPT but do cross the RR local QPT, i.e., the quantum quenches are from a conventional phase to the nearby GP [see Fig. 1(a)]. For those quenches, the RRs endow $Z(z)$ with YLF zeros arbitrarily close to the real-time axis. As in equilibrium GPs, these YLF zeros are spread over an area on the complex-time plane with the associated density of zeros depending on the details of the disorder variables in H [see Fig. 1(b)]. We thus propose the term dynamical quantum Griffiths phase to designate the real-time axis interval intersected by the YLF zeros [see Fig. 1(c)].

The reasoning behind our result is as follows. After the quench, the bulk remains nearly in its ground state since its

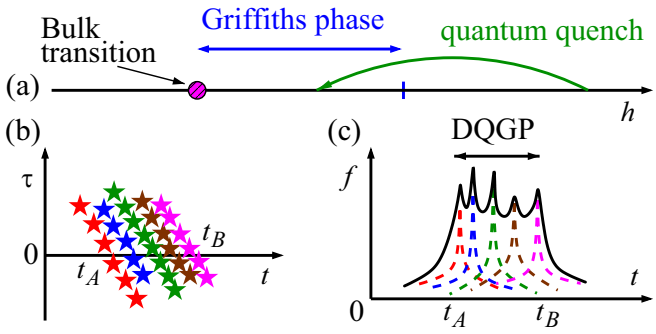

FIG. 1. Schematics of (a) the equilibrium phase diagram and the class of quantum quenches studied: from a point far from the quantum phase transition to a point in the nearby Griffiths phase. (b) The rare-region-induced zeros of the dynamical partition function Z, and (c) the associated dynamical free energy f (solid line). Each set of zeros (stars of a given color) and the corresponding dynamical free energy f_{RR} (dashed line) are due to a single rare region. The singular part of f is a simple superposition of all f_{RR}. The time window $t_A < t < t_B$ is the dynamical quantum Griffiths phase.

QPT was not crossed. The RRs, however, are highly excited. Because the RRs and the bulk are in different phases, these excitations do not rapidly decay. Thus, meanwhile, the RRs' dynamics is decoupled from the bulk's in a sense that will become precise later. Consequently, two sets of YLF zeros appear, one provided by the bulk and the other by the RRs. Those from the bulk are far from the real-time axis and thus only provide analytical contributions to $f(t)$. Those from the RRs, however, are arbitrarily close to the real-time axis and therefore are responsible for the nonanalyticities of $f(t)$. In addition, we show that this singular behavior can be well approximated by that of completely decoupled RRs with open boundary conditions undergoing the same quantum quench.

We remark that, differently from the known cases in the literature, the RRs in dynamical QPTs dominate the short-time dynamics. This is exciting because it allows for an easier identification of the RRs' effects in numerical studies and in experiments.

Finally, we notice that quenched disorder effects on dynamical QPTs were studied in a variety of models [39–44]. These studies, however, did not focus on the RR-induced effects.

In the remainder of this Letter, we derive our results from an explicit model Hamiltonian, discuss their generality and extensions, and provide concluding remarks.

Consider the transverse-field Ising chain

$$H = -\sum_{i=1}^{L} J_i \sigma_i^z \sigma_{i+1}^z - h \sum_{i=1}^{L} \sigma_i^x, \tag{2}$$

where $\boldsymbol{\sigma}_i$ are Pauli matrices, $J_i > 0$ are the ferromagnetic coupling constants (which, due to inhomogeneities, are site dependent), and $h > 0$ is the transverse field and plays the role of the tuning parameter of $H(h)$. We consider chains of L sites long with periodic boundary conditions $\boldsymbol{\sigma}_{L+i} = \boldsymbol{\sigma}_i$. The model has two zero-temperature phases: the ferromagnet ($h < h_c$) and the paramagnet ($h > h_c$) separated by a quantum critical point at $h_c = J_{\mathrm{typ}}$, where $J_{\mathrm{typ}} = e^{\overline{\ln J}}$ is the geometric mean of the coupling constants [45].

The clean system ($J_i = J$) can be solved analytically using standard methods [46]. The return probability amplitude (1) after the quantum quench $h_0 \to h$ (with $h_0 > h_c$) is

$$Z(z) = e^{-iE_0 z} \prod_{0<k_n<\pi} \left(1 - \frac{(1-\varepsilon_{k_n})(1-e^{-4i\omega_{k_n}(h)z})}{2}\right), \tag{3}$$

where $E_0 = -\sum_{n=1}^{L} \omega_{k_n}(h)$ is the ground-state energy of the postquench Hamiltonian, the momenta $k_n = (2n-1)\frac{\pi}{L}$, $n = 1, \ldots, L$, $\omega_k(h) = \sqrt{h^2 - 2hJ\cos k + J^2}$ is the dispersion relation, and $\varepsilon_k = \varepsilon_k(h, h_0) \equiv [hh_0 - J(h_0 + h)\cos k + J^2]/[\omega_k(h)\omega_k(h_0)]$. The YLF zeros of (3), $z^* = t^* + i\tau^*$, are

$$t^*_{m,n} = \frac{(2m+1)\pi}{4\omega_{k_n}(h)} \text{ and } \tau^*_n = \frac{\ln\left(\frac{1+\varepsilon_{k_n}(h,h_0)}{1-\varepsilon_{k_n}(h,h_0)}\right)}{4\omega_{k_n}(h)}, \tag{4}$$

where $m \in \mathbb{N}$ defines different accumulation lines of zeros (for a graphical illustration, see Supplemental Material [46]). These lines pierce the real-time axis if and only if the equilibrium QPT is crossed by the quantum quench, i.e., if and only if $(h - h_c)(h_0 - h_c) < 0$ in the model (2). In the following, we numerically demonstrate that even a single RR dramatically changes this scenario.

Unfortunately, there is no analytical solution for the nonhomogeneous case. We then compute $Z(z)$ in (1) via exact numerical diagonalization and find its YLF zeros z^* using the standard secant method [46]. For definiteness, we set the couplings in the Hamiltonian (2) to $J_i = J_{\mathrm{B}}$ (the bulk couplings) everywhere except inside a RR where $J_i = J_{\mathrm{RR}}$ for $1 \leqslant i \leqslant L_{\mathrm{RR}} - 1$. The fact that we are considering a compact RR is of no consequence for our purposes. Later, we discuss more general profiles. For simplicity, we consider quantum quenches from $h_0 = \infty$ to a finite h. Thus, $|\psi_0\rangle = \otimes_{i=1}^{L} |\rightarrow\rangle$, with $\sigma^x|\rightarrow\rangle = |\rightarrow\rangle$, is a simple product state. We want to study quenches that do not cross the bulk QPT, and thus $h > J_{\mathrm{B}}$. In the following numerical study, we set $h = 5J_{\mathrm{B}}$. Other values only produce quantitative changes and will be shown elsewhere.

We show in Fig. 2(a) the dynamical free energy for the homogeneous case $J_{\mathrm{RR}} = J_{\mathrm{B}}$ for a chain of only $L = 30$ sites long (for the sake of clarity) with periodic boundary conditions. The resulting curve (dotted line; notice it is multiplied by a factor of 10) is completely smooth and analytic as expected. The corresponding YLF zeros Eq. (4) are shown in Fig. 2(b) as open symbols. As is well known [26], they accumulate in lines far from the real-time axis. For the time window considered, only the first two accumulation (dashed) lines appear. Increasing J_{RR} gradually (in steps of $0.1h$ up to $3h$ and considering, for the sake of clarity, a rare region of only $L_{\mathrm{RR}} = 8$ sites long), the zeros move on the complex-time plane [see gray dots in Fig. 2(b)]. Analyzing their trajectories, we verify two distinct sets of zeros: one that remains in the upper half of the complex-time plane and the other which migrates to the vicinity of the real-time axis. The latter set of zeros accumulate in lines which pierce the real-time axis for $J_{\mathrm{RR}} > h$. For the case $J_{\mathrm{RR}} = 3h$, we plot the corresponding $f(t)$ in Fig. 2(a) (red solid line). The corresponding zeros are shown in Fig. 2(b) as solid symbols. The developing

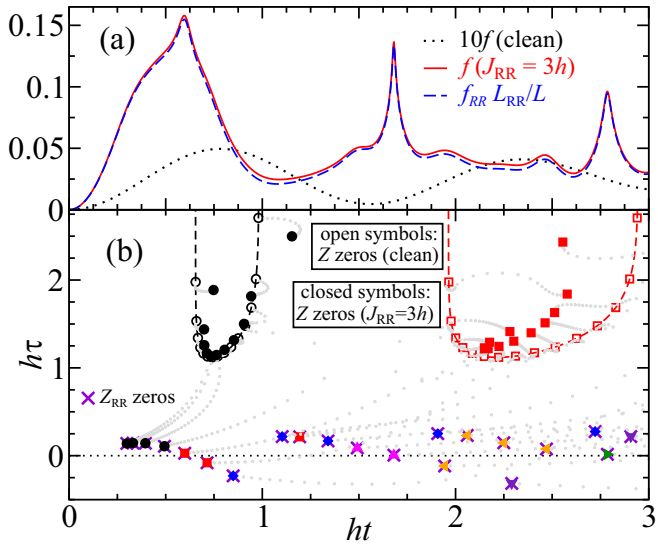

FIG. 2. (a) The dynamical free energy f as a function of the real time t for three different chains after the quantum quench from $h_0 = \infty$ to finite h. The first chain (black dotted line) is homogeneous, $L = 30$ sites long with periodic boundary conditions, and has couplings $J_B = h/5$. The second chain (red solid line) is identical to the first one except that it contains a RR of size $L_{RR} = 8$ inside which the couplings are $J_{RR} = 3h$. The third chain (blue dashed line) is homogeneous, L_{RR} sites long with open boundary conditions, and has couplings J_{RR}. (b) The corresponding Yang-Lee-Fisher zeros of $Z(z)$ for these three chains: open symbols, solid symbols, and $\times$ symbols, respectively. The zeros' trajectories of the second chain (when changing J_{RR} from $h/5$ to $3h$) are given by the gray dots (see text).

singularities in $f(t)$ are in one-to-one correspondence with the zeros close to the real-time axis.

Our interpretation of the latter set of zeros is that the unitary dynamics of the RR is essentially decoupled from the bulk. The reasoning is as follows. The bulk is gapful and is locally in a different phase from the RR. The RR excitations (kinks) have a different nature from the bulk's (spin flips). Therefore, the quench-induced excitations of the RR do not immediately decay into the bulk.

To give support to this interpretation, we compute the dynamical free energy f_{RR} and the corresponding YLF zeros of a decoupled RR with open boundary conditions undergoing the same quantum quench: the blue dashed line and violet $\times$ symbols in Figs. 2(a) and 2(b), respectively. We verify that $f_{RR}(t)$ accurately reproduces the singular part of $f(t)$, the difference being due to the analytical bulk's contribution. Interestingly, we verify a one-to-one correspondence between the set of zeros of $Z(z)$ near the real-time axis and the zeros of $Z_{RR}(z)$. The differences between them vanish exponentially as J_{RR} increases [46].

We now further explore the consequences of our interpretation: (i) Different RRs are independent (if sufficiently far from each other) and (ii) the postquench excitations are localized inside the RRs (for sufficiently short times). The reasoning behind (i) is because the bulk is practically in its ground state and thus its ground-state correlation length ξ is still a well-defined quantity.

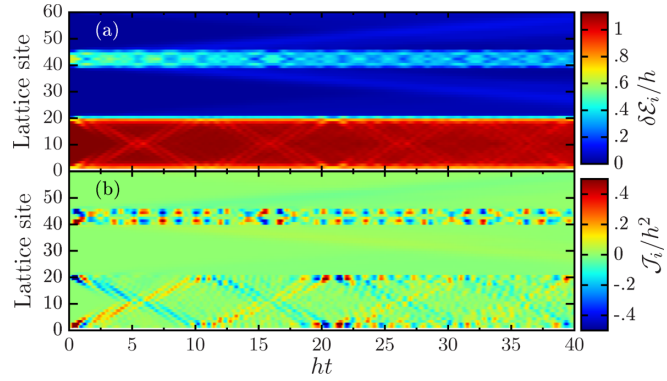

FIG. 3. (a) The mean energy density above the ground state $\delta\mathcal{E}_i$ and (b) the corresponding density current $\mathcal{J}_i$ as a function of the real time t for each lattice site i (see text).

To give evidence of the above statements, we study the time evolution of the mean energy density above the ground state $\delta\mathcal{E}_i = \langle\psi(t)|E_i|\psi(t)\rangle - \langle\phi_{GS}|E_i|\phi_{GS}\rangle$ (where $E_i = -\frac{1}{2}J_{i-1}\sigma^z_{i-1}\sigma^z_i - h\sigma^x_i - \frac{1}{2}J_i\sigma^z_i\sigma^z_{i+1}$ and $|\phi_{GS}\rangle$ is the ground state of the postquench H) and the associated density current $\mathcal{J}_i = hJ_{i-1}\langle\psi(t)| - \sigma^z_{i-1}\sigma^y_i + \sigma^y_{i-1}\sigma^z_i|\psi(t)\rangle$ [46]. We consider the same quench (from $h_0 = \infty$ to h) in a chain of $L = 60$ sites long with periodic boundary conditions where the bulk coupling is $J_B = 0.2h$. The chain has two RRs. One is 20 sites long with coupling constant $J_{RR,1} = 2h$, and the other is only 5 sites long with couplings $J_{RR,2} = 1.5h$. In Fig. 3, we plot the $\delta\mathcal{E}_i$ and $\mathcal{J}_i$ as a function of time.

Clearly, for the time window studied, the excitations are well localized inside the RRs and the bulk remains in its ground state carrying no energy current. We have also verified [46] that the singular part of $f(t)$ and the corresponding YLF zeros are well described by those of the same RRs undergoing the same quantum quench but decoupled from the bulk.

Having demonstrated that (i) the RR dynamics is effectively decoupled from the bulk and (ii) that the dynamics of sufficiently far apart RRs are essentially independent from each other, we can readily understand the origin and quantify the nonanalyticities of $f(t)$ for any quantum quench which does not cross the bulk QPT. All the singularities come from sufficiently large RRs which, independently, provide YLF zeros accumulating in lines piercing the real-time axis. Since the time instant in which these lines pierce the real-time axis depends on the microscopic details of the RRs, the YLF zeros will be generically distributed over an area of the complex-time plane. The intersection of this area with the real-time axis defines the dynamical quantum Griffiths phase (see Fig. 1).

Evidently, besides identifying the physical mechanism behind the nonanalyticities in $Z(t)$, it is also desirable to quantify it. From the Weierstrass factorization theorem, the singular part of $f(t)$ is [1,2,38]

$$f_{sing}(t) \propto \sum_{m,\alpha} \ln\left|t - t^*_{m,\alpha}\right| \to \int dt^* g(t^*) \ln|t - t^*|. \quad (5)$$

Here, $t^*_{m,\alpha}$ is the mth real-time YLF zero due to the αth RR. In the thermodynamic limit, the sum in Eq. (5) is replaced by

an integral weighted by the distribution of zeros $g(t^*)$. As noticed by Fisher [1], $f_{\rm sing}$ is as a two-dimensional electrostatic potential due to point charges at t^*. The nonanalyticity of $f(t)$ is thus encoded in the distribution $g(t)$, whose nonanalyticities are inherited from the distribution of the random variables in H. Naturally, an example that can be worked out analytically is desirable. This is provided by the percolating case in which the couplings are vanishing with probability p and equal to $J_\alpha > 0$ with probability $1-p$. Here, J_α is a random variable distributed according to $P(J)$. For the quantum quench $h_0 = \infty \to h = 0_+$, the dynamical free energy is [46]

$$f = -L^{-1}\sum_{k=1}^{L} \ln\cos^2(J_k t) \to -(1-p)\overline{\ln\cos^2(Jt)}, \quad (6)$$

where the thermodynamic limit was taken in the last passage and $\overline{(\cdots)} = \int dJP(J)(\cdots)$. The real-time YLF zeros are $t^*_{m,\alpha} = (2m_\alpha + 1)\pi/J_\alpha$. If J_α is uniformly distributed between J_1 and J_2, the nonanalyticities of $P(J)$ at $J = J_{1(2)}$ become nonanalyticities of $f(t)$ at the time instants $t^c_{m,1(2)} = (2m_{1(2)} + 1)\pi/J_{1(2)}$. Notice that these are the only time instants in which $f(t)$ is nonanalytic, even though there is a continuum of YLF zeros in the time window $t^c_{m,2} < t < t^c_{m,1}$. This is in close correspondence with the nonanalyticities of the electrostatic potential due to a continuous distribution of charges. The associated singularities are only log-infinite derivatives of f at the instants $t^c_{m,2}$ and $t^c_{m,1}$. At all other time instants, f is locally analytic. At first glance, this seems to imply a nearly undetectable nonanalytical behavior (just as classical Griffiths singularities). However, in numerical studies, the lack of a dense accumulation of real-time zeros yields a highly fluctuating free energy in that time window, as illustrated in Fig. 1(b). Different convergence schemes or precisions will produce highly different numerical results in the dynamical quantum Griffiths phase. We expect an analogous behavior in the current experiments [26,33–37] of ultracold atoms and other quantum simulators where the total number of degrees of freedom is far from the thermodynamic limit. In electrostatics, the same effect occurs if the probe of the electric field is able to distinguish between neighboring point charges. Mathematically, this is quantified by the Euler-Maclaurin formula of the difference between the sum and integral in Eq. (5), or, equivalently, by the difference between the sample average (sum) and the distribution average (integral) in Eq. (6).

In summary, we have shown that RRs play a fundamental role in the early-time dynamics of strongly interacting quantum systems after quantum quenches which cross the RR QPT but not the bulk QPT. In that case, the quench-induced excitations are confined in the RRs while the bulk remains nearly in its ground state. As a result, observables such as the dynamical free energy (1) become nonanalytic functions of time in the thermodynamic limit. The nonanalyticities are due to RR-induced YLF zeros accumulating in lines piercing the real-time axis. Evidently, it is desirable to know whether this situation applies to other model systems. For short times, we expect it to be quite general when the bulk is gapped since there will be infrequent resonances between the RRs and the bulk and thus the excitations remain confined. For a gapless bulk, the RR relaxation time may still be comparatively long since the nature of its excitations is fundamentally different from the bulk's. In other words, the quench-induced excitations in the RRs may not decay rapidly into the bulk due to the conservation of emergent quantum numbers. We stress that, counterintuitively, the RR-induced singular behavior of the dynamical free energy appears at short timescales. This fact makes the RR-induced singularities easier to be identified in numerical studies (such as time-dependent density matrix renormalization group) and in quantum simulator experiments (before the interactions with the environment spoil the unitary dynamics).

Notice that the nonequilibrium phenomenon here studied is of short timescales. Studying (the long-time physics of) thermalization after the quantum quenches here considered (when integrability-breaking terms are present) by quantifying how the excitations decay into the bulk and relating this to the position of the YLF zeros is an interesting task left for the future.

Finally, we remark that our results also apply to quantum annealing [47] from h_0 to h when the RR QPT is crossed. If the RR is sufficiently large or the annealing is sufficiently fast, excitations are generated and confined inside the RR. Thus, RRs play an important role for adiabatic quantum computing.

We acknowledge instructive discussions with M. Heyl, D. Luitz, R. Moessner, and M. Vojta. We also acknowledge the financial support of the Brazilian agencies FAPEMIG, FAPESP, and CNPq.

[1] M. E. Fisher, The nature of critical points, in *Lectures in Theoretical Physics*, edited by W. E. Brittin (University of Colorado Press, Boulder, 1965), Vol. VII C.

[2] C. N. Yang and T. D. Lee, Statistical theory of equations of state and phase transitions. I. Theory of condensation, Phys. Rev. **87**, 404 (1952).

[3] X. Peng, H. Zhou, B.-B. Wei, J. Cui, J. Du, and R.-B. Liu, Experimental Observation of Lee-Yang Zeros, Phys. Rev. Lett. **114**, 010601 (2015).

[4] K. Brandner, V. F. Maisi, J. P. Pekola, J. P. Garrahan, and C. Flindt, Experimental Determination of Dynamical Lee-Yang Zeros, Phys. Rev. Lett. **118**, 180601 (2017).

[5] A. B. Harris, Effect of random defects on the critical behaviour of Ising models, J. Phys. C: Solid State Phys. **7**, 1671 (1974).

[6] T. Vojta, Disorder-Induced Rounding of Certain Quantum Phase Transitions, Phys. Rev. Lett. **90**, 107202 (2003).

[7] J. A. Hoyos and T. Vojta, Theory of Smeared Quantum Phase Transitions, Phys. Rev. Lett. **100**, 240601 (2008).

[8] Y. Imry and S.-k. Ma, Random-Field Instability of the Ordered State of Continuous Symmetry, Phys. Rev. Lett. **35**, 1399 (1975).

[9] R. B. Griffiths, Nonanalytic Behavior Above the Critical Point in a Random Ising Ferromagnet, Phys. Rev. Lett. **23**, 17 (1969).

[10] B. M. McCoy, Incompleteness of the Critical Exponent Description for Ferromagnetic Systems Containing Random Impurities, Phys. Rev. Lett. **23**, 383 (1969).

[11] M. Wortis, Griffiths singularities in the randomly dilute one-dimensional Ising model, Phys. Rev. B **10**, 4665 (1974).

[12] A. B. Harris, Nature of the "Griffiths" singularity in dilute magnets, Phys. Rev. B **12**, 203 (1975).

[13] F. Iglói and C. Monthus, Strong disorder RG approach of random systems, Phys. Rep. **412**, 277 (2005).

[14] T. Vojta, Rare region effects at classical, quantum and nonequilibrium phase transitions, J. Phys. A: Math. Gen. **39**, R143 (2006).

[15] F. Iglói and C. Monthus, Strong disorder RG approach – a short review of recent developments, Eur. Phys. J. B **91**, 290 (2018).

[16] M. Randeria, J. P. Sethna, and R. G. Palmer, Low-Frequency Relaxation in Ising Spin-Glasses, Phys. Rev. Lett. **54**, 1321 (1985).

[17] A. J. Bray, Nature of the Griffiths phase, Phys. Rev. Lett. **59**, 586 (1987).

[18] A. J. Bray, Dynamics of Dilute Magnets above T_c, Phys. Rev. Lett. **60**, 720 (1988).

[19] M. J. Thill and D. A. Huse, Equilibrium behaviour of quantum Ising spin glass, Physica A **214**, 321 (1995).

[20] T. Vojta and J. A. Hoyos, Criticality and Quenched Disorder: Harris Criterion Versus Rare Regions, Phys. Rev. Lett. **112**, 075702 (2014).

[21] I. Bloch, J. Dalibard, and W. Zwerger, Many-body physics with ultracold gases, Rev. Mod. Phys. **80**, 885 (2008).

[22] I. M. Georgescu, S. Ashhab, and F. Nori, Quantum simulation, Rev. Mod. Phys. **86**, 153 (2014).

[23] P. Calabrese and J. Cardy, Time Dependence of Correlation Functions Following a Quantum Quench, Phys. Rev. Lett. **96**, 136801 (2006).

[24] A. Polkovnikov, K. Sengupta, A. Silva, and M. Vengalattore, Colloquium: Nonequilibrium dynamics of closed interacting quantum systems, Rev. Mod. Phys. **83**, 863 (2011).

[25] A. Mitra, Quantum quench dynamics, Annu. Rev. Condens. Matter Phys. **9**, 245 (2018).

[26] M. Heyl, A. Polkovnikov, and S. Kehrein, Dynamical Quantum Phase Transitions in the Transverse-Field Ising Model, Phys. Rev. Lett. **110**, 135704 (2013).

[27] F. Andraschko and J. Sirker, Dynamical quantum phase transitions and the loschmidt echo: A transfer matrix approach, Phys. Rev. B **89**, 125120 (2014).

[28] S. Vajna and B. Dóra, Disentangling dynamical phase transitions from equilibrium phase transitions, Phys. Rev. B **89**, 161105(R) (2014).

[29] M. Schmitt and S. Kehrein, Dynamical quantum phase transitions in the Kitaev honeycomb model, Phys. Rev. B **92**, 075114 (2015).

[30] J. C. Halimeh and V. Zauner-Stauber, Dynamical phase diagram of quantum spin chains with long-range interactions, Phys. Rev. B **96**, 134427 (2017).

[31] B. Žunkovič, M. Heyl, M. Knap, and A. Silva, Dynamical Quantum Phase Transitions in Spin Chains with Long-Range Interactions: Merging Different Concepts of Nonequilibrium Criticality, Phys. Rev. Lett. **120**, 130601 (2018).

[32] R. Jafari, Dynamical quantum phase transition and quasi particle excitation, Sci. Rep. **9**, 2871 (2019).

[33] P. Jurcevic, H. Shen, P. Hauke, C. Maier, T. Brydges, C. Hempel, B. P. Lanyon, M. Heyl, R. Blatt, and C. F. Roos, Direct Observation of Dynamical Quantum Phase Transitions in an Interacting Many-Body System, Phys. Rev. Lett. **119**, 080501 (2017).

[34] J. Zhang, G. Pagano, P. W. Hess, A. Kyprianidis, P. Becker, H. Kaplan, A. V. Gorshkov, Z.-X. Gong, and C. Monroe, Observation of a many-body dynamical phase transition with a 53-qubit quantum simulator, Nature (London) **551**, 601 (2017).

[35] H. Bernie, S. Schwartz, A. Keesling, H. Levine, A. Omran, H. Pichler, S. Choi, A. S. Zibrov, M. Endres, M. Greiner, V. Vuletić, and M. D. Lukin, Probing many-body dynamics on a 51-atom quantum simulator, Nature (London) **551**, 579 (2017).

[36] N. Fläschner, D. Vogel, M. Tarnowski, B. S. Rem, D.-S. Lühmann, M. Heyl, J. C. Budich, L. Mathey, K. Sengstock, and C. Weitenberg, Observation of dynamical vortices after quenches in a system with topology, Nat. Phys. **14**, 265 (2018).

[37] X.-Y. Guo, C. Yang, Y. Zeng, Y. Peng, H.-K. Li, H. Deng, Y.-R. Jin, S. Chen, D. Zheng, and H. Fan, Observation of a Dynamical Quantum Phase Transition by a Superconducting Qubit Simulation, Phys. Rev. Appl. **11**, 044080 (2019).

[38] Markus Heyl, Dynamical quantum phase transitions: a review, Rep. Prog. Phys. **81**, 054001 (2018).

[39] T. Obuchi and K. Takahashi, Dynamical singularities of glassy systems in a quantum quench, Phys. Rev. E **86**, 051125 (2012).

[40] C. Yang, Y. Wang, P. Wang, X. Gao, and S. Chen, Dynamical signature of localization-delocalization transition in a one-dimensional incommensurate lattice, Phys. Rev. B **95**, 184201 (2017).

[41] H. Yin, S. Chen, X. Gao, and P. Wang, Zeros of Loschmidt echo in the presence of Anderson localization, Phys. Rev. A **97**, 033624 (2018).

[42] V. Gurarie, Dynamical quantum phase transitions in the random field Ising model, Phys. Rev. A **100**, 031601(R) (2019).

[43] K. Cao, W. Li, M. Zhong, and P. Tong, Influence of weak disorder on the dynamical quantum phase transitions in the anisotropic XY chain, Phys. Rev. B **102**, 014207 (2020).

[44] U. Mishra, R. Jafari, and A. Akbari, Disordered Kitaev chain with long-range pairing: Loschmidt echo revivals and dynamical phase transitions, J. Phys. A: Math. Theor. **53**, 375301 (2020).

[45] P. Pfeuty, An exact result for the 1D random Ising model in a transverse field, Phys. Lett. A **72**, 245 (1979).

[46] See Supplemental Material at http://link.aps.org/supplemental/10.1103/PhysRevB.106.L140201 for technical details and a description of our numerical approach, which includes Refs. [48–50].

[47] B. Gardas, J. Dziarmaga, W. H. Zurek, and M. Zwolak, Defects in quantum computers, Sci. Rep. **8**, 4539 (2018).

[48] D. S. Fisher, Critical behavior of random transverse-field Ising spin chains, Phys. Rev. B **51**, 6411 (1995).

[49] E. Lieb, T. Schultz, and D. Mattis, Two soluble models of an antiferromagnetic chain, Ann. Phys. **16**, 407 (1961).

[50] A. P. Young and H. Rieger, Numerical study of the random transverse-field Ising spin chain, Phys. Rev. B **53**, 8486 (1996).